# Sussing Merger Trees: Stability and Convergence

Yang Wang,[1,2,3,4]* Frazer R. Pearce,[2] Alexander Knebe,[5,6] Aurel Schneider,[7,8]
Chaichalit Srisawat,[7] Dylan Tweed,[9,10] Intae Jung,[11] Jiaxin Han,[12]
John Helly,[12] Julian Onions,[2] Pascal J. Elahi,[13] Peter A. Thomas,[7]
Peter Behroozi,[14,15] Sukyoung K. Yi,[16] Vicente Rodriguez-Gomez,[17]
Yao-Yuan Mao,[14,15] Yipeng Jing,[10] and Weipeng Lin[1,3]

[1] *School of Physics and Astronomy, Sun Yat-Sen University, Guangzhou, 510275, China*
[2] *School of Physics & Astronomy, University of Nottingham, Nottingham, NG7 2RD, UK*
[3] *Key Laboratory for Research in Galaxies and Cosmology, Shanghai Astronomical Observatory, Shanghai 200030, China*
[4] *Graduate School of the Chinese Academy of Science, 19A, Yuquan Road, Beijing, China*
[5] *Departamento de Física Teórica, Módulo 15, Facultad de Ciencias, Universidad Autónoma de Madrid, 28049 Madrid, Spain*
[6] *Astro-UAM, UAM, Unidad Asociada CSIC*
[7] *Department of Physics and Astronomy, University of Sussex, Brighton BN1 9QH, UK*
[8] *Institute for Computational Sciences,University of Zurich, Switzerland*
[9] *Racah Institute of Physics, The Hebrew University, Jerusalem 91904, Israel*
[10] *Center for Astronomy and Astrophysics, Department of Physics, Shanghai Jiao Tong University, Shanghai 200240, China*
[11] *Department of Astronomy, The University of Texas at Austin, Austin, TX, 78712, USA*
[12] *Institute for Computational Cosmology, Department of Physics, Durham University, South Road, Durham DH1 3LE, UK*
[13] *Sydney Institute for Astronomy, A28, School of Physics, The University of Sydney, NSW 2006, Australia*
[14] *Kavli Institute for Particle Astrophysics and Cosmology and Physics Department, Stanford University, Stanford, CA 94305, U SA*
[15] *SLAC National Accelerator Laboratory, Menlo Park, CA 94025, USA*
[16] *Department of Astronomy and Yonsei University Observatory, Yonsei University, Seoul 120-749, Republic of Korea*
[17] *Harvard-Smithsonian Center for Astrophysics, 60 Garden Street, Cambridge MA, 02138, USA*

**ABSTRACT**

Merger trees are routinely used to follow the growth and merging history of dark matter haloes and subhaloes in simulations of cosmic structure formation. Srisawat et al. (2013) compared a wide range of merger-tree-building codes. Here we test the influence of output strategies and mass resolution on tree-building. We find that, somewhat surprisingly, building the tree from more snapshots does not generally produce more complete trees; instead, it tends to shorten them. Significant improvements are seen for patching schemes which attempt to bridge over occasional dropouts in the underlying halo catalogues or schemes which combine the halo-finding and tree-building steps seamlessly. The adopted output strategy does not affect the average number of branches (bushiness) of the resultant merger trees. However, mass resolution has an influence on both main branch length and the bushiness. As the resolution increases, a halo with the same mass can be traced back further in time and will encounter more small progenitors during its evolutionary history. Given these results, we recommend that, for simulations intended as precursors for galaxy formation models where of order 100 or more snapshots are analysed, the tree-building routine should be integrated with the halo finder, or at the very least be able to patch over multiple adjacent snapshots.

**Key words:** methods: numerical – galaxies: haloes– galaxies: evolution – dark matter

## 1 INTRODUCTION

In the current standard cosmological model, galaxies are thought to form and evolve within the potential well of a surrounding dark matter halo (White & Rees 1978; Efstathiou & Silk 1983; Blumenthal et al. 1984). Gas assembly and star formation takes place within this environment, and the hierarchical merging of the haloes gives rise to galaxy mergers. The whole life of a galaxy is intimately connected to this underlying host halo framework.

Thus, when undertaking galaxy modeling, a set of appropriate

* wangyang23@mail.sysu.edu.cn

haloes and their associated merger tree histories are a key ingredient. One leading approach for this task is using Semi-Analytic Models (SAMs). The merger trees employed by SAMs can be derived from the Press-Schechter formalism (Press & Schechter 1974) or extended Press-Schechter formalism (Bond et al. 1991), or in a more realistic way directly from $N$-body simulations (see Roukema et al. (1997); Lacey & Cole (1993) for the historical origin of both approaches). The latter approach has become popular since $N$-body simulations can provide more realistic halo histories in complex environments. Although merger trees derived from $N$-body simulations are widely used, their performance and properties have not been thoroughly studied to date. This was the aim of our SUSSING MERGER TREES workshop[1] from which arose a series of comparisons studying various aspects of merger trees.

Srisawat et al. (2013) was the first paper from the SUSSING MERGER TREES workshop. It gave a general overview on the contributing merger-tree-building methods. As we found, different tree codes produce distinctly different results. Following up this work, Lee et al. (2014) found that for SAMs, the $z = 0$ galaxy properties are altered if different halo merger-tree-building algorithms are used. The star formation history and the properties of satellite galaxies can be remarkably different. They also showed that these changes could be largely alleviated if the model was re-tuned to the input tree. This work demonstrated that different tree building algorithms construct different merger trees, which cannot all reflect the true structure of the underlying dark matter halo framework they are purporting to encapsulate. Thus although re-tuning is possible this is not an ideal situation. In this paper we attempt to quantify the differences between the different algorithms by varying both the simulation output strategy and the simulation resolution.

Besides this general view, we are also interested in any aspects that will affect merger tree construction. Basically there are two steps for building merger trees. First we need an input halo catalogue which is usually found by employing a halo finding code on every snapshot. Then these catalogues of haloes from each snapshot are linked together by a tree-building code to construct a merger tree. Since the input halo catalogue can be varied when different halo finding codes are applied, it is natural that the input halo catalogue can affect the final merger trees. Avila et al. (2014) found that the underlying halo finder is very relevant to the merger trees built. Different underlying halo catalogues result in changes to the main branch length and the branching ratio of the resultant merger trees.

In this work, we explore fundamental aspects that influence merger tree construction. We test whether our 9 contributing tree-building algorithms can recover stable and convergent merger trees when the simulation output strategy is changed and discuss an optimal strategy. This work contains two parts: first we test merger tree stability by changing the output frequency of the underlying simulation; we follow this by testing convergence by changing the mass resolution of the simulation. We study the performance of the various merger tree builders under these changes in the numerical input conditions.

The rest of this paper is organized as follows: we start by describing the simulation data we have used and list the merger tree building codes applied in Section 2. We then define the properties we measure for our merger trees in Section 3. Our main results are given in Sections 4, 5 and 6, followed by a discussion and some conclusions in Section 7.

---

## 2    SIMULATION DATA AND MERGER TREE BUILDERS

### 2.1    Stability study

The first simulation is a dark-matter-only re-simulation of a Milky Way-like halo taken from the Aquarius project (Springel et al. 2008, hereafter SINGLEHALO). Specifically we use Aquarius halo A at level 4, which has a mass resolution of $M_{\rm p} = 2.868 \times 10^5 {\rm M}_\odot$. For the Aquarius project the underlying cosmology is $\Omega_M = 0.25$, $\Omega_\Lambda = 0.75$, $\sigma_8 = 0.9$, $h = 0.73$. Because this simulation is a single halo re-simulation, most of the haloes at redshift 0 (which will be the root haloes of our merger trees) are subhaloes. Only a few of them are distinct haloes.

In total the simulation outputs 1024 snapshots (given IDs 0 to 1023 sequentially from the earliest snapshot to the final one) from redshift 50 to 0. We subsample the full output set in order to undertake our merger tree stability study. This study attempts to quantify the effects of varying the output strategy on the resulting merger tree. To test this, we extract specific snapshots from the original output set of the SINGLEHALO simulation. There are 5 sets for analysis:

• Using all 1024 snapshots. This forms the Thousand Output (TO) dataset.

At the beginning of the simulation the time interval between output snapshots is about $4.5 \times 10^5$ years. This slowly increases with time and reaches $1.9 \times 10^7$ years at snapshot 440 (where the redshift of 2.93). After that the time interval remains constant at $1.9 \times 10^7$ years.

• Using every 4th snapshot from the full TO set, i.e. the 4th, 8th, 12th ... 1024th snapshot. There are 256 snapshots in this set, which forms the Quarter Output (QO) dataset.

• Selecting 64 outputs matching the Millennium simulation output strategy, which are equally spaced in log expansion factor at high redshift. This set forms the Millennium Output (MO) dataset. The time interval for this set is $\Delta \ln a \approx 0.081$, where $a$ is the expansion factor, at high redshift. It gradually decreases with time and reaches a value of $\Delta \ln a \approx 0.020$ by $z = 0$.

• Selecting 64 outputs equally spaced in time. This set forms the Equally timed Output (EO) dataset. The time interval for this set is about $2.7 \times 10^8$ years.

• A set of 64 outputs deliberately selected to be a poor choice. In this case we select pairs of adjacent snapshots followed by a large gap, particularly at early times. At late times the gaps reduce and there are more neighbouring snapshots. This set forms the Lame Output (LO) dataset.

These five output strategies are displayed visually in Figure 1, which illustrates the spacing of the various snapshots as a function of cosmic time and expansion factor. Expanded timelines for the TO and LO datasets are inserted to illustrate the many snapshots in the base TO simulation and the pairing of snapshots in the LO dataset.

### 2.2    Convergence study

To study the behaviour of merger trees with mass resolution we have also run two dark matter-only simulations with the same initial conditions and cosmology, but at a different resolution. They each follow the evolution of structure in a small box of comoving side $8h^{-1}$ Mpc containing $512^3$ particles (hereafter the HIRES simulation) and $256^3$ particles (hereafter the LORES simulation), respectively. The resolution is $m_p = 2.1 \times 10^6 \ h^{-1} {\rm M}_\odot$ for LORES simulation and $m_p = 2.6 \times 10^5 \ h^{-1} {\rm M}_\odot$ for HIRES simulation.
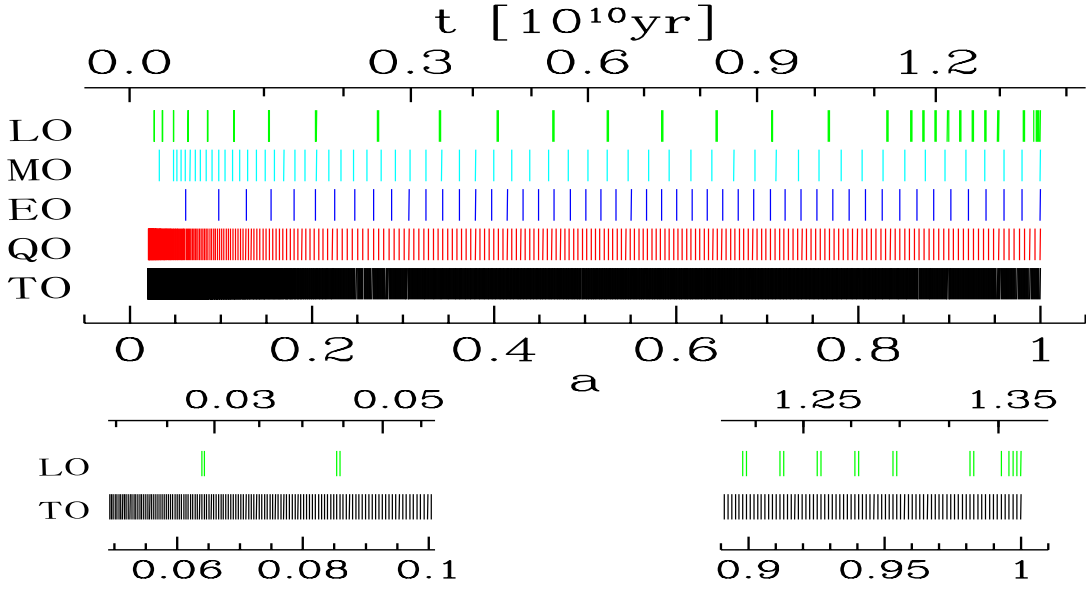
**Figure 1.** Output scheme for all five datasets. The horizontal axis lists both the expansion factor $a$ and cosmic time $t$. A vertical bar in a specific position indicates a snapshot at the corresponding time. Each set of vertical lines illustrates one dataset, as listed on the left. In the lower part, two zoom in regions are shown for the Thousand Output(TO) and Lame Output(LO) datasets.

Their mass resolution is equivalent to the resolution of the Aquarius project simulations at level 5 and level 4, respectively (Springel et al. 2008). The mass resolution of the Aquarius simulation at level 5 is roughly three times higher than that of the Millennium-II simulation ($m_p = 6.9 \times 10^6 \, h^{-1} M_\odot$) used by Lee & Lemson (2013). The cosmology was chosen to be the same as in the Aquarius simulation, i.e. $\Lambda$CDM with $\Omega_M = 0.25$, $\Omega_\Lambda = 0.75$, $\sigma_8 = 0.9$, $n_s = 1$, $h = 0.73$. Initial conditions were generated at $z = 127$ using the Zel'dovich approximation to linearly evolve positions from an initially glass-like state. This was then evolved to the present day using GADGET-2 (Springel 2005) with a gravitational softening equal to $0.04 h^{-1}$kpc. Both simulations output 51 snapshots. We study the appearance of the merger trees that result from these two simulations which only differ in mass resolution.

In contrast to the stability study, the two simulations used in our convergence study are full box cosmological simulations. They contain populations of both main haloes and subhaloes. Since the convergence of merger trees concerns mergers of haloes, cosmological simulations are more appropriate for this study.

### 2.3 Description of tree builders

We employ nine different algorithms to build merger trees in this work. In this section we briefly list the contributed tree builders. For this work we supplied a single (sub)halo catalogue generated by SUBFIND (Springel et al. 2001) in order to ensure consistency for the halo generation step. A comparison of the effect of different halo finding algorithms on the resultant trees has already been completed by Avila et al. (2014). We asked each of the tree building teams to construct merger trees based on this input halo catalogue. HBT and to some extent CONSISTENT TREES are slightly different from other tree-builders on this point in that they add subhaloes while building the merger tree, and in effect edit the halo population.

All of the tree-builders except JMERGE trace the haloes via individual particle IDs which are matched between snapshots. They link two haloes together if they share the same particles and can meet the requirement of a merit function. Their merit functions are somewhat different (refer to Srisawat et al. (2013) for further details). The nine supplied algorithms split into 4 broad types:

- **Class 1:** Example: JMERGE (Onions). This simplest type aims to build merger trees from simulation datasets which do not include particle IDs. They only require the halo mass and trajectory to match haloes with their progenitors.
- **Class 2:** Examples: MERGERTREE (Knollmann & Knebe 2009; Gill et al. 2004), TREEMAKER (Tweed et al. 2009), VELOCIRAPTOR (Elahi et al. 2011), ySAMTM (Jung et al. 2014). The simplest tree-building algorithms that make use of particle IDs to assist halo matching between snapshots. They only use adjacent snapshots and do not attempt to correct the resultant trees for any defects in the halo catalogue or halo dropouts. Since their results are almost indistinguishable, we label them as CLASS2 codes.
- **Class 3:** Examples: SUBLINK (Rodriguez-Gomez et al. 2015), D-TREES (Jiang et al. 2014), CONSISTENT TREES (Behroozi et al. 2013). These are more sophisticated algorithms that attempt to patch the constructed trees by searching for matches over several snapshots. They will search one or more steps further if they can't find the progenitors in consecutive snapshots. CONSISTENT TREES will also insert 'fake' progenitors when it feels that there are missing ones, and it uses additional information such as the gravitational motion of haloes in determining progenitor matches.
- **Class 4:** Example: HBT (Han et al. 2012). This class of tree builder tracks haloes and subhaloes throughout the simulation, intimately connecting the halo finding step with the tree-building stage. First it takes a friends-of-friends halo catalogue as an input catalogue. It tracks haloes from the first snapshot in which they appear, and adds their descendants to the subhalo population if they are accreted and survive.

For a detailed description of each of these tree-building codes please refer to section 4 of Srisawat et al. (2013) and the appropriate individual methods papers.
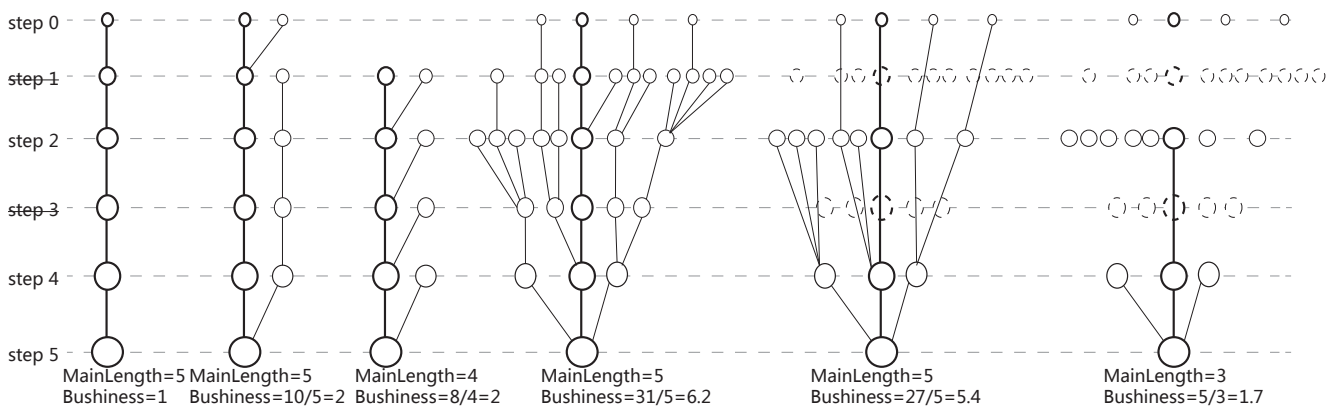
**Figure 2.** Calculation of main branch length $L$ and bushiness $B$ as defined in the text for 6 example trees. The thick line represents the main branch. If snapshots are dropped to form a smaller dataset then the fourth tree can become the fifth or the sixth depending on whether or not the progenitor branches are well linked. The sixth tree has a significantly reduced bushiness.

## 3  ANALYSED MERGER TREE PROPERTIES

### 3.1  Merger tree geometry

Quantifying the merger tree geometry is fundamental to further analysis. Such physical properties are derived from the structure of the merger tree. In this work, two main properties are used to describe the merger tree geometry: the length of the main branch (hereafter $L$) and the average number of branches of the merger tree (hereafter referred to as the bushiness, $B$). In previous work in this series, the main branch length and the branching ratio (the number of direct progenitors of a halo) were used to characterize a merger tree. Here the branching ratio is replaced with bushiness, because the former will introduce bias to any comparison between merger trees with different numbers of snapshots and snapshot intervals. A uniform parameter, such as bushiness, circumvents this issue.

The length of the main branch illustrates how far a halo can be traced back in time through a succession of snapshots. In this work, $L$ is defined as the difference between the IDs of the snapshot of the root and the snapshot of the earliest main progenitor. Note that we fix the snapshot IDs within the full TO dataset and preserve these numbers when selecting a subset of snapshots to produce the other four datasets that make up the stability analysis. A detailed definition of what forms the main branch and other terminology used here can be found in section 2 of Srisawat et al. (2013).

The bushiness of a merger tree is a measure of its average number of branches. It is defined as the sum of the length of all the connections that form the tree divided by the length of the main branch. A connection is a link between two nodes, i.e. a link between a halo in the merger tree and one of its direct progenitors. The difference between the IDs of the snapshots which contain the two nodes is the length of this connection. As before, the original snapshot ID from the TO dataset is used in this calculation so that this parameter can be compared among different sets.

Figure 2 illustrates the calculation of main branch length and bushiness. The fifth and sixth trees (from the left) show how the main branch length and bushiness of the fourth tree changes when the output strategy is changed by dropping the indicated snapshots. Assuming that snapshots 1 and 3 are dropped from the tree, if a tree builder retained the ability to link progenitors despite the missing snapshot, the fourth tree will become the fifth. However, if progenitor branches cannot be accurately linked the tree can collapse to the sixth tree. The main branch is shown as the thick line in the middle of each tree.

Figure 2 illustrates how the average tree bushiness is calculated in practice. For example, the 4th tree has 31 connections all of length unity and a main branch length of 5, resulting in a bushiness of $31/5 = 6.2$. For the fifth tree, the tree builder has worked well and reconstructed a structure similar to the full tree. There are 15 connections, 12 of length two and 3 of unit length, for a total value of 27. The main branch retains length 5 and the bushiness is almost unchanged at 5.4. However, for the much reduced sixth tree, there are only 4 recovered connections, one of length two and three of unit length, for a total value of 5. The main branch length is also smaller at 3. The bushiness of this tree is hence reduced to 1.7. In general, a merger tree with larger bushiness has more connections with respect to its main branch and appears wider and more complex. A low bushiness implies a thin tree, dominated by the main branch.

### 3.2  Physical properties

The mass assembly history (MAH) of haloes provides an important constraint on models of galaxy formation. We investigate the build-up of mass within the trees as a function of cosmic time by measuring the total mass within tree main branches at each snapshot, normalized to the mass at $z = 0$. This parameter illustrates how far back the mass assembly history can be traced (see also, Jiang et al. 2014).

The merger rate is another important physical property in galaxy formation. A galaxy's shape, metallicity and colour may be affected by merger events. Thus, as they form the underlying framework, the mergers of haloes also need to be considered. In this work, we study both mergers between haloes and mergers between subhaloes. Haloes more massive than $10^8 M_\odot$ are taken into account. We calculate the mean merger number per descendant halo per Gyr as a function of redshift. This parameter has been widely used in many works investigating the mergers of dark matter haloes and galaxies (see, e.g., Fakhouri & Ma 2008, 2009; Fakhouri et al. 2010; Genel et al. 2009, 2010).

It should be clarified that, particularly when aggregated, the merger rate and the bushiness are related but not identical properties of a set of merger trees. A larger bushiness implies that a merger tree has more sub-branches per unit length, while a larger merger
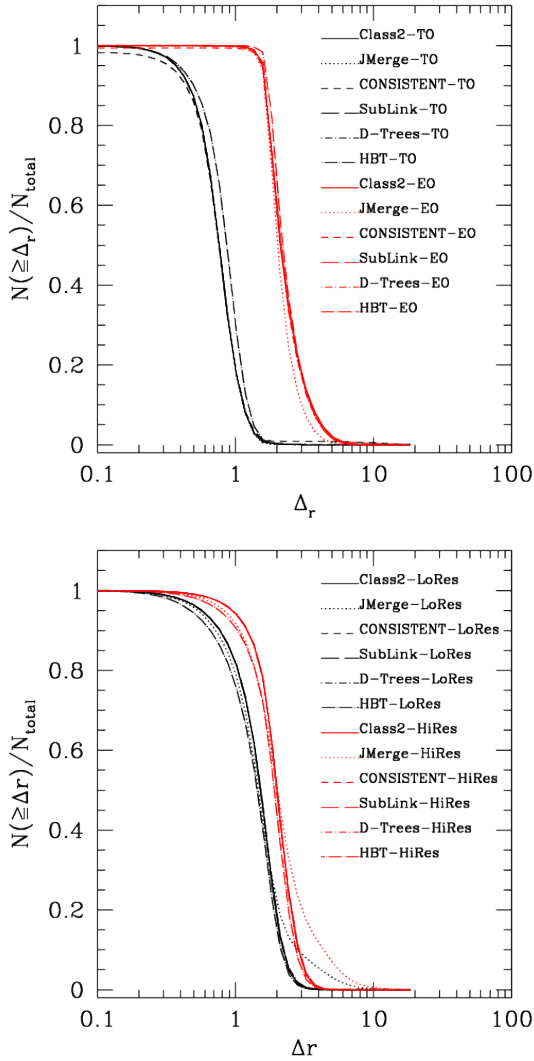
**Figure 3.** The displacement statistic, $\Delta r$ (see text), for all haloes and their main progenitors for which both have more than 200 particles. The upper panel displays results from the SINGLEHALO simulation. For brevity only the TO (black lines) and EO (red lines) output strategies are displayed. The lower panel displays results for the convergence study. Black lines are from the LORES simulation and red lines are from HIRES simulation. In both panels the different styles of line represents different tree-builders.

rate similarly implies more mergers per unit time. However, the precise time-step at which a merger is counted varies between the two properties because subhalo trees are not connected to the host halo tree until the subhalo has been effectively destroyed by the host halo. Hence the number of progenitors is not directly equivalent to the number of mergers on any particular step.

## 4 RESULT I: CONSISTENCY TEST

Before discussing the properties of merger trees, we want to ensure that every tree builder works appropriately for the different output strategies and mass resolutions. Here we use the following merit function, known as the *displacement statistic*, to quantify the performance of merger trees:

$$\Delta_r = \frac{|\mathbf{r}_B - \mathbf{r}_A - 0.5(\mathbf{v}_A + \mathbf{v}_B)(t_B - t_A)|}{0.5(R_{200A} + R_{200B} + |\mathbf{v}_A + \mathbf{v}_B|(t_B - t_A))}. \tag{1}$$

Here subscripts $A$ & $B$ refer to the two snapshots being compared, $t$ is the cosmic time, $\mathbf{v}$ and $\mathbf{r}$ are the velocity and position of the considered (sub)halo and its progenitor, and $R_{200}$ is the radius that encloses an overdensity of 200 times the critical density. Srisawat et al. (2013) used this formula to quantify how far haloes are displaced from their expected locations when moving from one snapshot to the next. Large values indicate a halo mismatch in the tree. It should be mentioned that Srisawat et al. (2013) only employed this statistic for the deviation of main haloes because it is hard to predict the motion of subhaloes. In this work we simply compare the values of $\Delta_r$ arising from the various tree-building codes and therefore we also include subhaloesin our analysis.

As the upper panel of Figure 3 shows, most lines from the same output strategy (with the same colour but different line style) overlap, although the value of the turnover, which corresponds to the peak in Figure 6 of Srisawat et al. (2013) is larger. This is due to the inclusion of subhaloes whose locations are harder to predict. The result for HBT (long dash-dotted line) is to some extent different from the others, because HBT alters the underlying halo catalogue. We have verified for all output strategies that the distributions from different builders also agree well. For brevity only lines from TO and EO are shown in the figure.

The lower panel of Figure 3 shows the same statistic, $\Delta_r$, for both the HIRES and LORES simulations. As we saw previously, lines for the different codes overlap in both simulations (except JMERGE, the dotted line). As discussed in Srisawat et al. (2013), JMERGE occasionally makes incorrect halo matches due to the lack of particle ID information. The difference between the LORES and HIRES result can be attributed to the very large difference in the number of subhaloes. The HIRES simulation has more subhaloes than the LORES simulation which makes $\Delta_r$ larger.

We conclude that varying the output strategy (even dramatically in the case of the LO dataset) or changing the mass resolution does not break any of the contributed merger-tree-building routines and that they all produce results in line with our expectations.

## 5 RESULT II: STABILITY OF MERGER TREE

### 5.1 Geometry

Figure 4 shows the cumulative main branch length function for the various output datasets as indicated in each panel. We examine merger trees of root haloes with 20-100 particles, 100-500 particles and more than 500 particles. For brevity, we only display the results for haloes with 20-100 particles and more than 500 particles here. The results from haloes with 100 to 500 particles are close to those from haloes with more than 500 particles. For class 2 tree-builders without patching, such as MERGERTREE, TREEMAKER, VELOCIRAPTOR, and YSAMTM, the results are almost indistinguishable, so we plot them on a single subplot labelled CLASS2.

For the thousand output dataset (TO), most codes find shorter main branches, hence producing lower curves on the plots. This is due to additional snapshots increasing the probability of cutting a link. The rising trend of the curves from the quarter output (QO), equal timed output (EO) and Millennium output (MO) supports this conclusion. This effect is very clear for small haloes, and for large haloes when class 2 tree-builders without patching are applied. Patching the merger tree by using information from additional snapshots clearly alleviates this problem to a greater or lesser
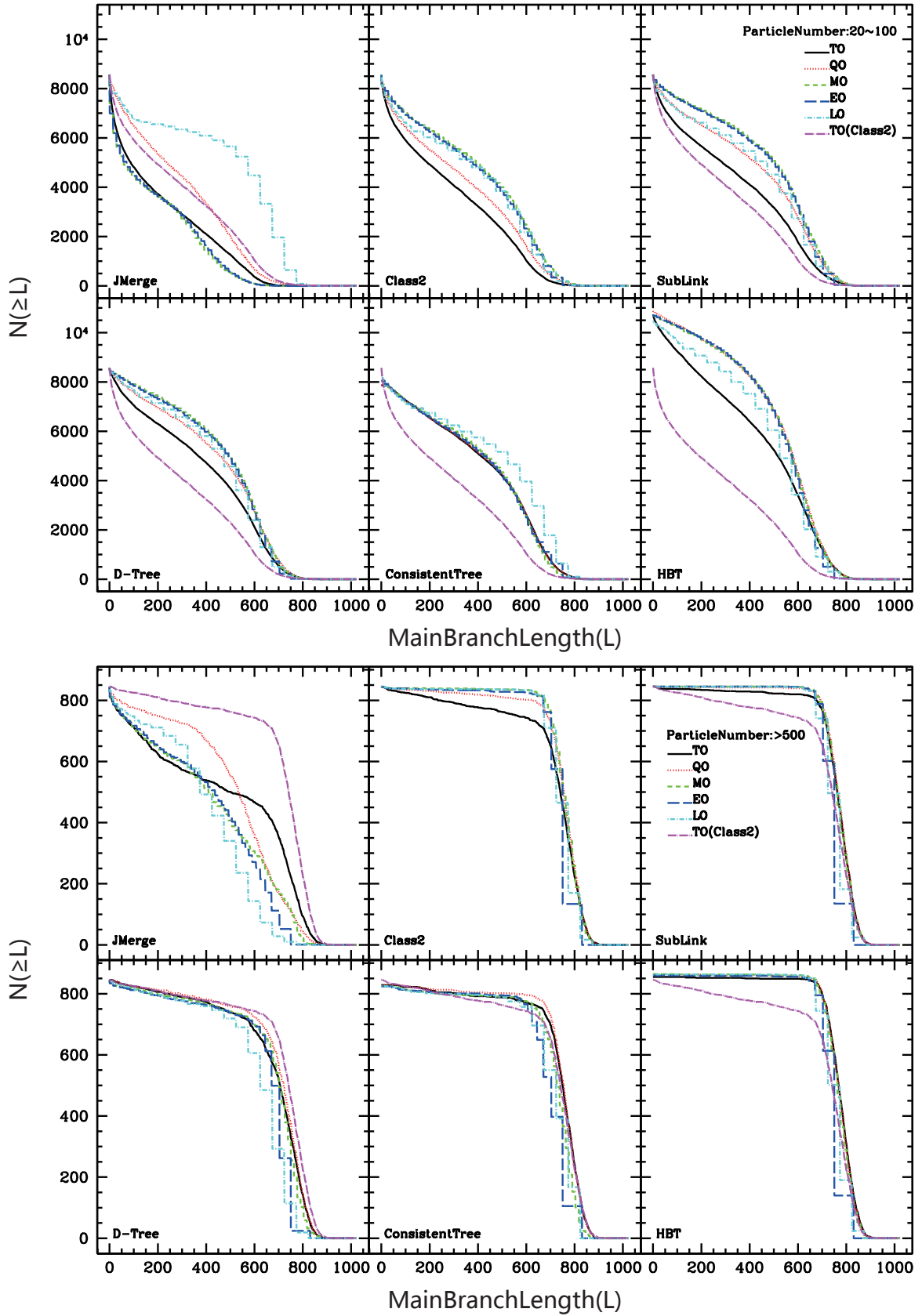
**Figure 4.** Cumulative number of merger trees with main branch lengths larger than $L$ in the SINGLEHALO simulation. The upper panel with 6 subplots shows the results from merger trees with root haloes containing 20-100 particles, and the lower panel is for root haloes larger than 500 particles. Each subpanel shows the results of a tree-builder as labeled in the bottom left corner. Different line colours and styles represent different output strategies as indicated in the legend. The TO line of CLASS2 is reproduced in magenta on all panels for guidance.

extent (we show three examples of class 3 builders that achieve this). Of the three shown here, CONSISTENT TREES is the most stable to changes in the output strategy, with almost overlapping results. Both SUBLINK and D-TREES could probably be adapted to achieve this too. However, by default they interpolate over a (small) fixed number of snapshots rather than over a fixed time-scale. For both of them the number of patching snapshots needs to be increased in proportion to the number of outputs, something that was not done here.

The class 4 builder, HBT, also shows stable performance for merger trees with large root haloes. It finds very long main branch lengths and the curves of all output datasets overlap when building trees for haloes with more than 100 particles. However, it finds a somewhat low TO line for halos with 20-100 particles. We suggest that the additional snapshots increase the probability of cutting a link, because some haloes may not easily be resolved by the halo finder. A halo could be unresolvable if it falls into a larger halo, or if its mass fluctuates taking it below the minimum particle number threshold of the halo finder. Class 3 builders can handle this situation by patching over the unresolved halo. However, HBT does not do any patching. It finds descendants just in the next snapshot. Its unique algorithm allows it to track subhaloes accurately but it can still lose track when a main halo fluctuates to too a small size. The latter situation happens more for main haloes with a small number of particles.

In all the panels the curves of MO and EO are generally almost indistinguishable. This implies that small differences in the interval between outputs do not affect the merger tree too much, especially when such differences occur in the early stages of the simulation.

The lame output strategy LO causes problems for the class 1 tree builder because wildly changing time intervals between snapshots makes extrapolation of halo positions to enable matching very difficult. The LO dataset does not cause too many problems for the class 2 tree builders, although in some cases the LO lines are slightly lower than those of the EO and MO datasets. For small haloes with the class 3 patching tree builders, this difference becomes clearer. This implies that the unconventional output strategy LO may prevent the patching process from optimizing the merger tree.

Using our CLASS3 routines we can identify how many haloes are being missed in the CLASS2 methods by noting when the CLASS3 methods patch the tree by inserting an extra halo. We show this in Figure 5, which gives the fraction of patched haloes for SUB-LINK, D-TREES & CONSISTENT TREES for the TO output set. All haloes are taken into account in this figure. We see that for all three methods at least 1 percent of the haloes are required to be patched at all times and that this fraction rises at early times. Conversely, without patching, at least 1 percent of the haloes are missed from the trees at all times. We have tested the dependency of this missing fraction with the number of snapshots used. From 1 percent for the TO, the fraction rises slowly as the number of snapshots is reduced, roughly doubling for the 64 snapshot strategies, i.e. about 2 percent of haloes are missed by the 64 output strategies, MO & EO at $z = 0$.

Figure 6 shows that, with the exception of JMERGE, the bushiness of the trees does not change for different output strategies. We only show trees with root haloes larger than 500 particles here, since the results for the other ranges are similar. This result indicates that the merger history is rarely affected by the output strategy and that in terms of bushiness all the class 2, 3 & 4 merger-tree-builders produce trees that look very similar. The exception is
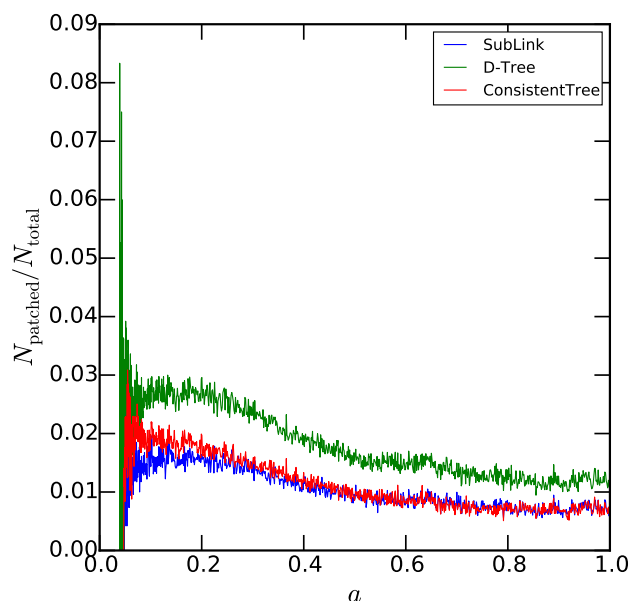


**Figure 5.** The fraction of patched haloes in every snapshot in the TO dataset as a function of the scale factor, $a$. Each line represents a different CLASS3 tree builder as indicated.

JMERGE which produces both significantly more very bushy trees (i.e. trees with very short main branches compared to the number of branches), as well as significantly more 'bare' trees that consist almost entirely of the main branch. These differences can again be attributed to the difficulty in matching haloes between snapshots when no particle ID information is available, a consequence of which is oddly shaped trees.
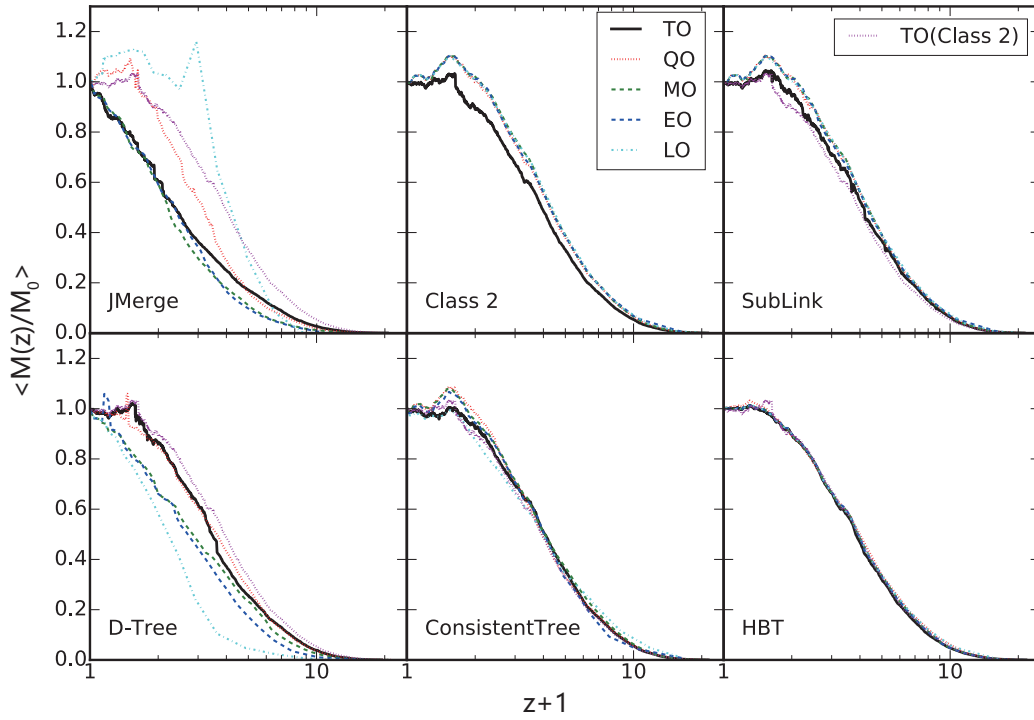
### 5.2 Mass history

Figure 7 illustrates the mass history for haloes between $0.5 \times 10^9 M_\odot$ and $1.5 \times 10^9 M_\odot$ at $z = 0$, normalized by the mass contained within this set at $z = 0$. The different line styles indicate the different output sets as detailed in the legend. This confirms the results seen earlier for main branch length which indicated that most of the builders find less material within haloes for the TO output set compared to the sets with fewer outputs. JMERGE again struggles in comparison to all the builders that use particle IDs, with a dramatic growth in haloes at late times due to the very truncated trees this method often produces. HBT produces extremely stable results by this measure, as was indicated to some extent by Figure 4.

We study individual tree mass histories in Figure 8. In this figure we compare 5 haloes' merger trees across the different output sets and tree builders. Each column shows one halo's mass accretion history and each row shows the merger trees constructed by the same tree builder as indicated. The matched HBT (sub)haloes' have different IDs because HBT constructs its own halo catalogue. Different line styles represent different output sets as indicated on the legend. The lines from the TO set are in bold so that the TO output can easily be distinguished from the other sets. In row 2, which shows the mass growth of merger trees built by CLASS2 tree builders, we see several examples of the cutting of the main branch in the TO output set.

Rapid declines in mass and violent fluctuations are also seen for many tree builders. These typically arise due to mergers, where
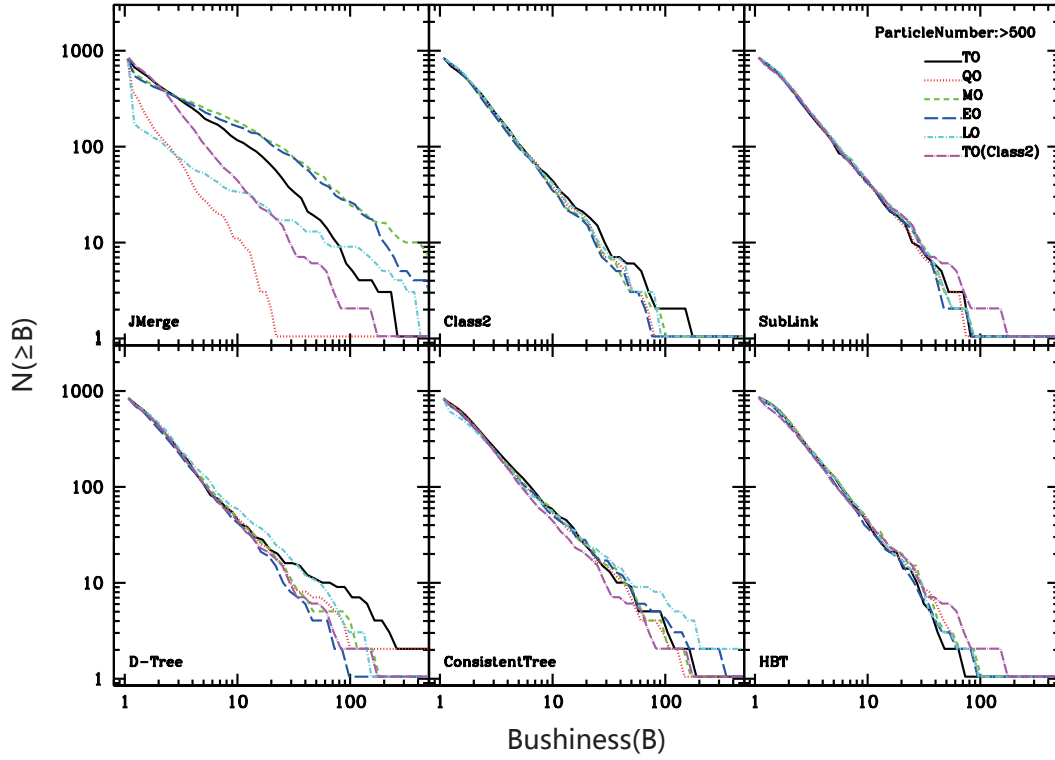
**Figure 6.** Merger tree bushiness $B$ for each of the builders in SINGLEHALO simulation. Only root haloes with more than 500 particles are selected here. Each subpanel shows results for an individual tree-builder as indicated, except for the four class 2 finders which are indistinguishable and are therefore all shown on the same subpanel. Different line colours and styles represent different output strategies as indicated in the legend. The CLASS2 TO line is reproduced on all panels for guidance.



**Figure 7.** Average mass history for each of the builders as a function of redshift. This corresponds to the total mass in tree main branches for root haloes between $0.5 \times 10^9 \mathrm{M_\odot}$ and $1.5 \times 10^9 \mathrm{M_\odot}$ at $z = 0$, normalized by the mass at $z = 0$. Different lines represent merger trees built from different output strategies, as indicated by the legend. Each subpanel displays results for one tree builder as indicated, except for the four class 2 finders which are indistinguishable and so are all shown on the same subpanel. The TO line of CLASS2 is reproduced in magenta on all panels for guidance.
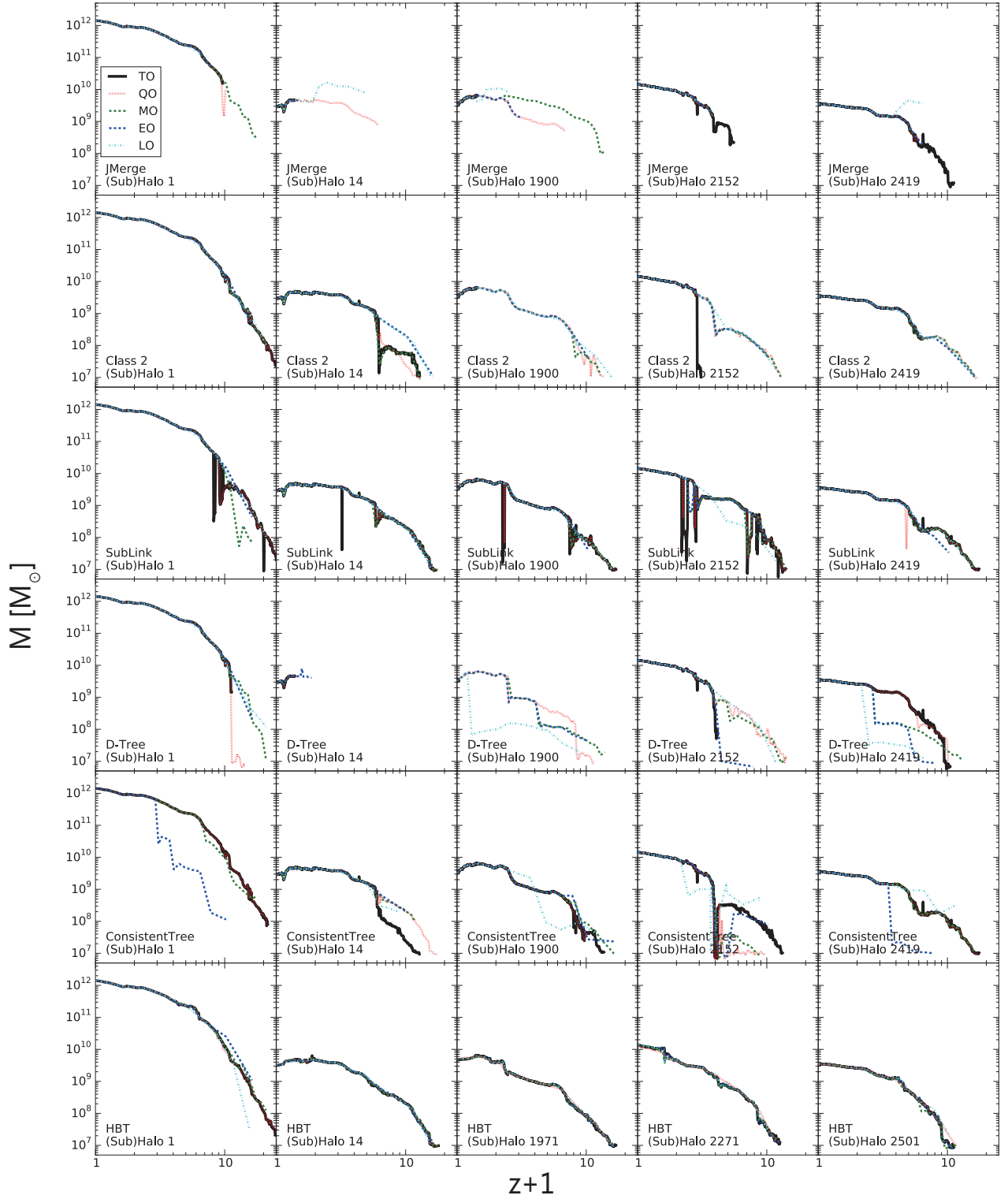
**Figure 8.** Mass histories for 5 (sub)haloes constructed by different merger-tree-builders. Different line styles represent different output strategies, as shown by the legend. Each row shows results for one tree builder as indicated, except for the four CLASS2 finders which are indistinguishable and so are all shown on the second row.
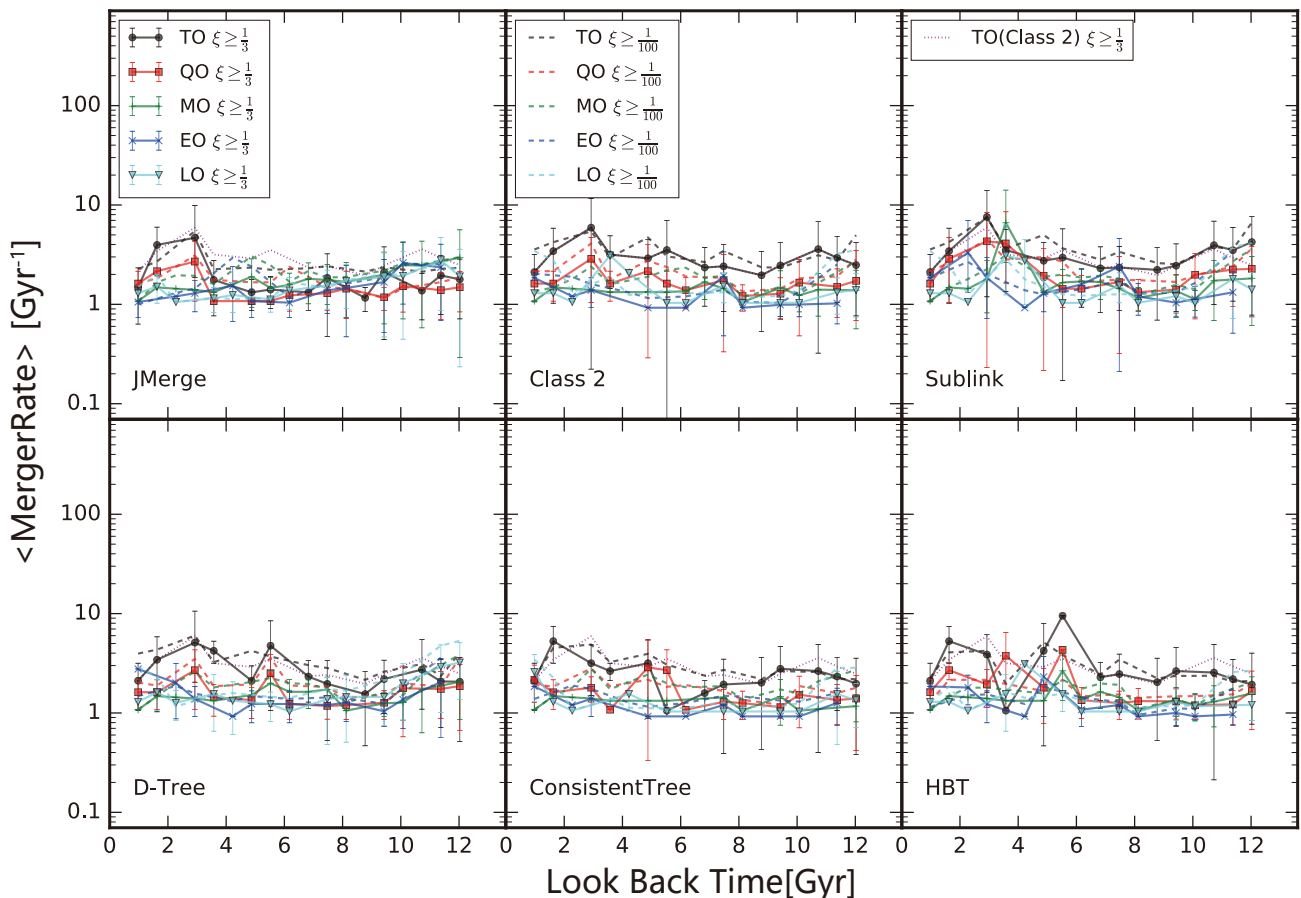
**Figure 9.** Mean merger rate (mergers per descendant halo per Gyr) as function of look-back time. Lines with different colour represent the merger tree built with a different output strategy, as shown by the legend. Solid lines show the merger rate with progenitor mass ratio larger than $1/3$. Dashed lines show the merger rate with progenitor mass ratio larger than $1/100$. The TO line of CLASS2 is reproduced in magenta on all panels for guidance. The error bars show the rms in every time bin. Each subpanel shows results for one tree builder as indicated, except for the four class 2 finders which are indistinguishable and so are all shown on the same subpanel.

distinguishing haloes and assigning masses becomes difficult, as reported by Srisawat et al. (2013) and Avila et al. (2014). Behroozi et al. (2015) explore this issue further by studying the consequences of major merger events.

Figure 8 can also help us understand how to implement patching algorithms which aim to bridge over the drop-outs particularly seen for the CLASS2 builders. Such patching may also aim to smooth over the rapid and unphysical mass fluctuations seen here. As can be seen in Figure 8 the class 3 tree builders we have tested all work to some extent, although some issues remain for some haloes. For example for halo 14 we see an illustration of the reappearance of a halo for the D-TREES finder (second column). D-TREES also has issues with halo 1900 (third column). We stress that we could have found similar examples for all the class 3 builders and that such instances are far less common for the class 3 builders compared to CLASS2. As expected the bottom row of Figure 8, which shows merger trees built by HBT, is relatively stable. HBT constructed its own (sub)halo catalogue during the process of building its merger trees. This extra work suggests that a good starting halo catalogue is an important factor in constructing merger trees.

For more information about comparing the influence of the input halo catalogue, see Avila et al. (2014).

### 5.3 Merger rate

Figure 9 shows the mean merger rate as function of look-back time (in units of Gyr). Haloes with $z = 0$ masses between $(1 \pm 0.5) \times 10^9 M_\odot$ are selected. When calculating the merger rate, the number of merger events is divided by the time interval over which this number of mergers are seen. Because the time interval between snapshots can be quite small, this can lead to unstable merger rate. In this case multiple snapshots are aggregated. For consistency, the time interval is fixed. In the EO output set, it is $0.81 \text{Gyr}$. In the other sets, the time interval varies from $0.8 \text{Gyr}$ to $1.05 \text{Gyr}$, because the snapshots cannot be exactly matched.

As for our earlier results for bushiness, in Figure 9 we show that the mean merger rate for each output set is essentially indistinguishable. Given the similarity between these two measures this is not entirely surprising. It is interesting that the Class 3 and Class 4 finders that include patching are not significantly different from the CLASS2 finders. In practice mergers are readily detectable and

although some 'flyby' events may be misclassified as mergers, the number of such events is small.

The merger rate shown in Figure 9 is different from Figure 8 in Fakhouri & Ma (2008). This is because in SINGLEHALO most haloes are subhaloes, Figure 9 actually shows the merger rate of subhaloes.

## 6 RESULT III: CONVERGENCE OF MERGER TREE

### 6.1 Geometry

Figure 10 shows the cumulative number of trees with main branch lengths larger than $L$ in the LORES and HIRES simulations. To investigate the influence of resolution, we draw two lines for comparison: trees with root haloes containing more than 500 particles in the LORES box (black solid line), and equivalent trees with root haloes containing more than 4000 particles in the HIRES box (green dashed line). This choice corresponds to haloes more massive than $10^9 M_\odot$ in both simulations. The green dashed line represents the same halo population as the black solid line, simulated at higher resolution. The comparison between the black line and the green line indicates that, for trees with the same root halo mass range, better mass resolution results in longer main branches. All the codes perform alike except for JMERGE which appears to show the opposite trend. For trees with smaller root haloes the trends are similar to Figure 10, though the deviation between the green line and the black line is larger. We can also see that patching class 3 and higher tree builders still find slightly longer main branches than the class 2 builders in both simulations (the CLASS2 curves are overplotted on the other panels in blue and cyan for comparison).

Figure 11 shows that resolution will also affect the bushiness of the merger trees. The peak of the green line shifts right compared to the black line, indicating that haloes with the same mass have bushier trees in the higher resolution simulation. As seen previously, all the codes perform alike except for JMERGE which is resolution independent unlike all the other builders. In practice two factors drive an increase in bushiness: either there is a dramatic decrease in the main branch length or an increase in the number of secondary branches leading to an increase in the number of merger events. Since we have seen that the main branch length becomes larger with increasing resolution, we can rule out the first of these. Rather, the increased resolution leads to an increase in the number of minor mergers and hence the measured bushiness of the trees, an effect that outweighs the slightly longer length of the main branches.

To test this, we plot Figure 12 to look into the details of progenitors. We select haloes with more than one progenitor from all snapshots, and plot the number of progenitors against their mass. Since all codes (except JMERGE) look alike in Figure 11, changes due to the resolution make little difference among the tree builders. So we only plot Figure 12 for MERGERTREE. The images for the other builders (except JMERGE) are very similar. The letters $A_l$, $A_h$, $B_l$, & $B_h$ in the figure refer to four specific haloes we chose to investigate. $A_l$ and $B_l$ are haloes in the LORES box, $A_h$ is halo $A_l$ in the HIRES box and $B_h$ is halo $B_l$ in the HIRES box.

Here we introduce the terms 'major progenitor' and 'minor progenitor' to aid the description. If a progenitor's mass is more than 33 percent of its descendant's, we call it a major progenitor; otherwise, we call it a minor progenitor. We separate these two kinds of progenitors in the statistic. The lower panel of Figure 12
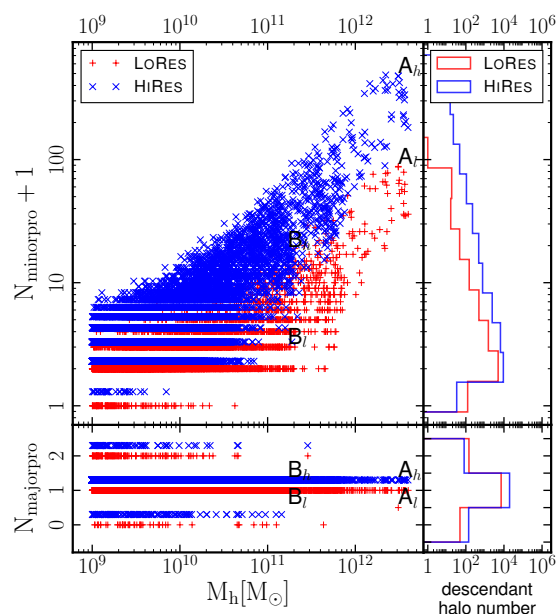


**Figure 12.** The number of progenitors a halo has as a function of its mass and histogram of the number of progenitors. The left lower panel counts the number of major progenitors, which have a mass larger than one third of their descendants', and the left upper panel counts the number of minor progenitors, which have a mass smaller than one third of their descendants'. Red pluses represent haloes from the LORES simulation and green crosses represent haloes from the HIRES simulation. The right lower panel represents the histogram of the number of major progenitors, and the right upper panel represents the histogram of the number of minor progenitors. Red lines indicate the LORES simulation and green lines indicate the HIRES simulation. All haloes from all snapshots with more than one progenitor are included. For clarity, points from the HIRES simulation are shifted up slightly.

shows that the number of major progenitors does not change due to the resolution, while the number of minor progenitors shifts to higher values in the HIRES box. In the subplots to the righthand side, we plot the histogram of the numbers of major and minor progenitors in the different resolutions. This figure gives yet another result: although the bushiness, which is equivalent to the average number of progenitors throughout a halo's evolutionary history, is affected by the resolution, increasing the resolution will only increase the number of minor progenitors.

The increase in minor progenitors is mainly due to the fact that we can resolve smaller mass (sub)haloes in the higher resolution simulation. This is a problem that chiefly concerns halo finding itself rather than the merger-tree-builder. We compared the location of the progenitors of halo $A_l$ and halo $A_h$, to halo $B_l$ and halo $B_h$. While their number increases, none of these small progenitors can be matched in position. In the non-linear regime much of the small scale structure is totally different even if two simulations share the same initial condition. This is a general issue beyond the scope of this paper so we will not discuss it further here.

### 6.2 Mass history

As for Figure 7, Figure 13 shows the mass history for haloes in the two simulations. Except for JMERGE, all the tree builders find similar mass histories, with a bulge in the HIRES simulation due to higher mass resolution. This is consistent with the geometry inves-
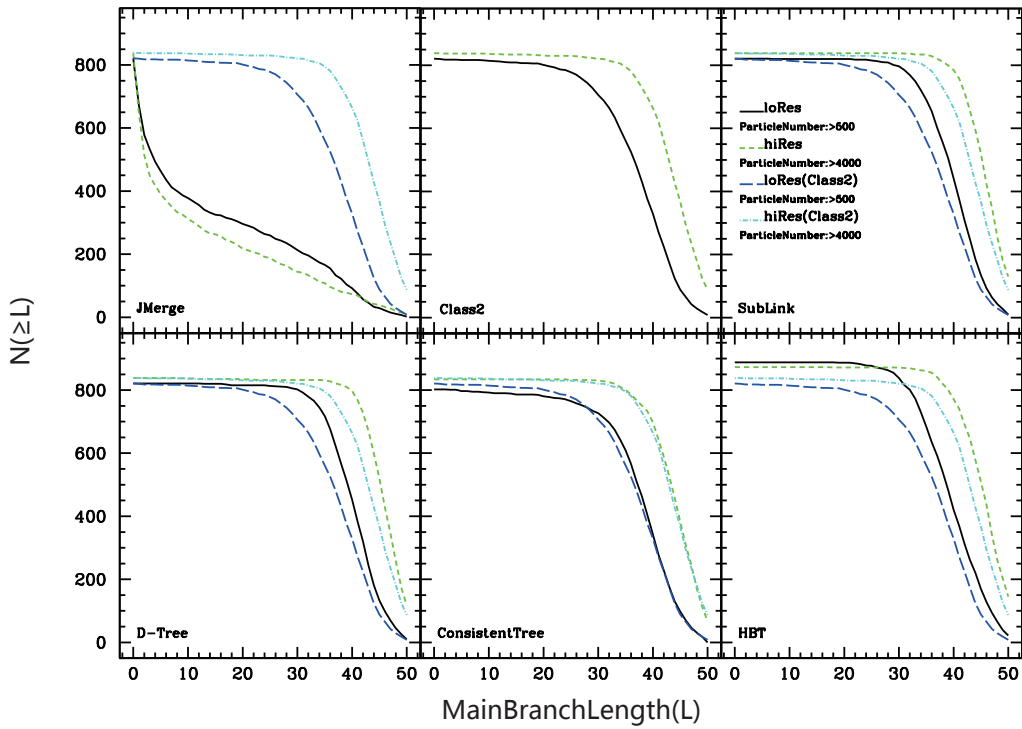
**Figure 10.** Cumulative number of trees with main branch lengths larger than $L$ in the LoRes and HiRes simulations. Root haloes with 20-100 particles in the LoRes simulation are selected. Trees with root haloes with the same particle number or the same halo mass in the HiRes simulation are selected respectively. Each panel represents one tree builder as indicated except for the four class 2 builders which are shown together on the Class2 panel. Different line types and colours represent different datasets as indicated in the legend.The LoRes and HiRes lines of Class2 is reproduced in blue and cyan on all panels for guidance.
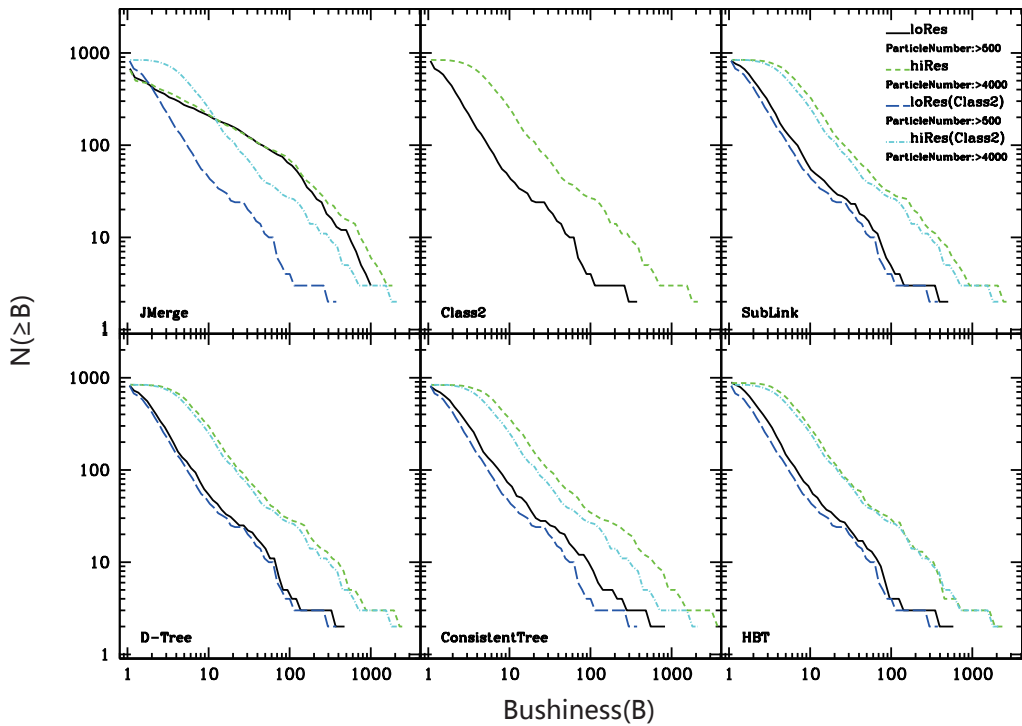


**Figure 11.** Number of trees of each bushiness $B$ in the LoRes and HiRes simulations. The criterion for selection and the linetypes are the same as for Figure 10

tigation. In the HIRES simulation, the smaller (sub)haloes extend the merger trees to earlier times, which results in a longer main branch. JMERGE again shows dramatic mass accretion into trees at late times, a result of the many broken main branches in produces.

## 6.3 Merger rates

Figure 14 shows the mean merger rate in the LORES and HIRES simulations. Haloes with mass in the range of $(1 \pm 0.5) \times 10^9 M_\odot$ are selected. All the tree builders, except JMERGE, find very similar mean merger rates for progenitor ratios larger than $1/3$. In the HIRES simulation they also find slightly higher mean merger rates for progenitor ratios larger than $1/100$. This suggests that in the HIRES simulation, the merger rate increases slightly due to the increased number of small haloes, in agreement with Figure 11, which showed that the HIRES simulation has a larger bushiness. JMERGE produces a higher merger rate because it sometimes links the wrong progenitor to descendant halo, an act which mimics a merger.

## 7 DISCUSSION AND CONCLUSIONS

Following our first paper (Srisawat et al. 2013) and a series of articles comparing various aspects of merger tree-building codes, we utilized nine different algorithms to investigate the influence of output strategy and resolution on the quality of the resulting merger trees.

The output strategy mainly affects the main branch length of the constructed merger trees. As our results show, somewhat counterintuitively, increasing the number of outputs from which the tree is generated results in shorter trees. This is because, due to limitations in the input halo catalogue, tree-builders may face difficulties caused by the fluctuating center and size (see for instance Srisawat et al. (2013), Figure 4) of the input haloes. During merging events some haloes may even disappear completely and then reappear again in a later snapshot (e.g. Behroozi et al. (2015), Figure 4). This ambiguous identification will happen more frequently if there are more snapshots, and this will increase the chance of terminating a tree main branch prematurely. This issue is not so prevalent for all our algorithms. It is particularly bad for class 1 type builders such as JMERGE which lack particle information to aid the halo identification. All four of our class 2 finders suffer significant problems as the number of snapshots is increased with halo main branches becoming shorter and shorter. Of the class 3 finders, where attempts are made to patch over gaps in the halo history by looking at additional snapshots, the stability of the reconstruction is varied. Both SUBLINK and D-TREES show some residual dependence on snapshot number while CONSISTENT TREES is essentially independent of the number of outputs. HBT is somewhat different, as it is a tracking finder that interleaves the halo finding and tree-building stages. This generates a different final halo catalogue which contains more haloes. While the MO, EO and QO output strategies display very similar results, the full TO dataset has a somewhat different dependence due to the HBT method losing track of small main haloes with such finely spaced outputs.

We also explore the influence of output strategy on bushiness, a measure of the average number of branches a tree has. We reach the conclusion that this property changes little with output strategy even though the corresponding main branch length fluctuates.

Our mass resolution study indicates that, as expected, tree-builders will build slightly longer trees for haloes with the same mass in a higher resolution simulation. This is true for all our algorithms except JMERGE where the additional haloes found at higher resolution introduce confusion due to the lack of particle ID tracking which acts to shorten the main branch length. The numerical resolution of the simulation has a larger influence on the bushiness of the derived merger trees: higher resolution results in larger bushiness. This extra bushiness results from the minor progenitors of haloes, as Figure 12 shows. The number of major mergers does not change too much. This result is to be expected because, in a low resolution simulation, very small haloes cannot be resolved by the halo finder. In a higher resolution simulation these small haloes appear and are linked to the branches of the merger tree, resulting in an increase of the main branch length and the bushiness of the tree. This resolution dependency mostly comes from the resolution limitation of the input halo catalogue rather than the tree-builders themselves. This results in all tree-builders, except JMERGE, producing very similar results.

As well as investigating the merger tree geometry we also looked into the mass history and merger rate of our trees. We found, as for the main branch length, that mass accretion was slightly lower with many outputs because some trees have been ended prematurely by occasional dropouts in the halo catalogues. The mass history was slightly boosted in the higher mass resolution simulation, since the finely resolved small haloes could extend the trees branches to higher redshifts. The merger rate is analogous to bushiness and was also largely independent of output strategy.

Our results show that patching schemes can improve merger trees. They also show that complete halo catalogues play an important role in building merger trees. Such an influence of the input halo catalogue on merger-tree-building has been discussed by Avila et al. (2014). In this work, we allowed CONSISTENT TREES and HBT to modified the initial halo catalogue because it's part of their algorithm. Thus CONSISTENT TREES and HBT show the influence of both a patching scheme and changing the input halo catalogue at the same time.

To conclude, the simulation output strategy chiefly effects the main branch length of the resultant merger trees. The underlying simulation's resolution has an effect on both the length and bushiness of the merger trees. We recommend:

- Halo merger-tree-builders that do not consider the particle IDs should be avoided. They construct trees that do not reflect the underlying cosmological model accurately, having an incorrect merger rate and typical object age, for example.

- As has been found previously by Srisawat et al. (2013), all four of our class 2 finders, which do not attempt to patch the underlying merger tree, are functionally identical. They differ in terms of the details of the merit function used to connect haloes when building the tree. Although this choice makes occasional minor differences such that the trees produced are not actually identical, these differences are to all intents and purposes irrelevant.

- Merger trees built from of order 100 or more snapshots should always be constructed using an algorithm capable of dealing with problems in the underlying halo finder such as missing haloes. This patching should ideally be based on a physical timescale rather than a fixed number of snapshots and this timescale should be chosen to exceed the timescale over which haloes typically disappear for.

- To facilitate this patching at the end of the simulation, snapshots should be generated *beyond* the desired endpoint. This would entail typically running past $z = 0$. Also, without patching we have shown in Figure 5 that any halo catalogue will be incomplete
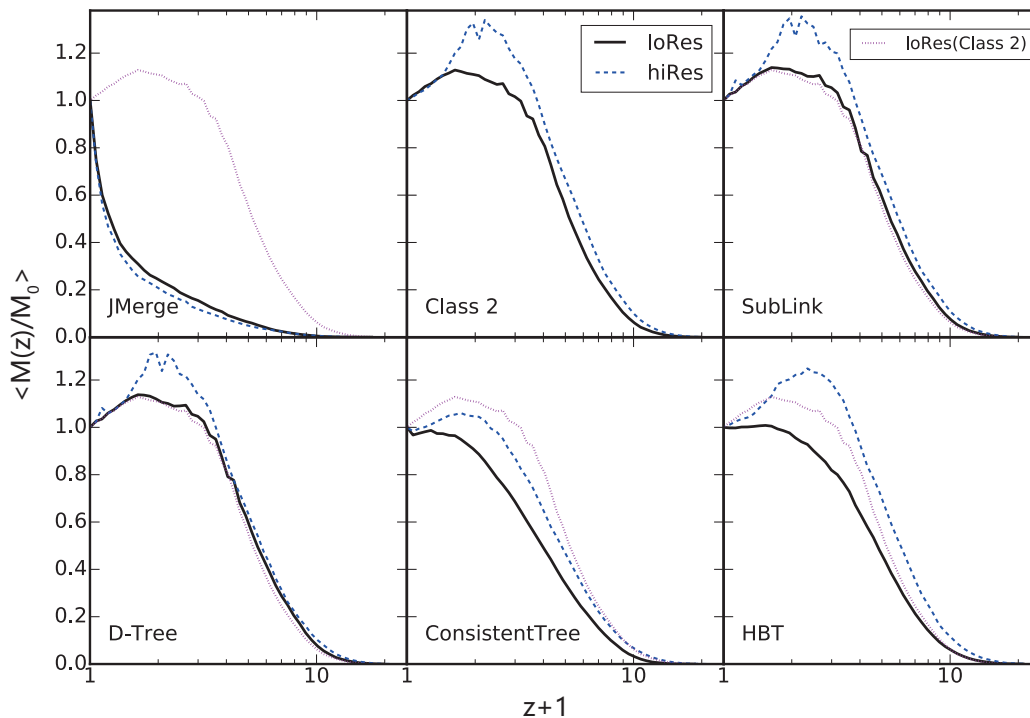
**Figure 13.** Average mass history for each of the builders as a function of redshift. Total mass in tree main branches for root haloes between $0.5 \times 10^9 M_\odot$ and $1.5 \times 10^9 M_\odot$ at $z = 0$, normalized by the mass at $z = 0$. Different line styles represent the merger trees built in the HIRES and LORES simulations, as shown by legend. Each subpanel displays results for one tree-builder as indicated, except for the four class 2 finders which are indistinguishable and so all shown on the same subpanel. The TO line of CLASS2 is reproduced in magenta on all panels for guidance.

at least at the 1 percent level, rising to 2 percent for 64 snaphots. This may be an issue for precision work.

• Sequences of snapshots with very rapidly changing time intervals between them should be avoided as they can lead to very poor trees.

• CLASS2 finders, which do not attempt to patch input halo catalogues, construct merger trees whose main branches are somewhat shorter than those that could be achieved if patching was applied. As such the merger trees produced do not accurately reflect the true structure of the underlying cosmological model. This can be important if the generated merger tree is to be subsequently used by a semi-analytic model, even though, as Lee et al. (2014) found, SAMs can be re-tuned to adjust for an incomplete tree structure (as this effectively necessitates tuning to an incorrect cosmology). Well constructed tree-builders capable of bridging incomplete halo catalogues or ideally fully integrated tracking finders of class 3 or 4 are therefore preferred.

The authors contributed in the following ways to this paper: YW & FRP designed the comparison and performed the analysis. YW is a PhD student supervised by WPL. YW & FRP wrote the paper. PAT, CS, AK, FRP & AS organized the Sussing Merger Trees workshop at which this work was initiated. The other authors (as listed in section 2.3) provided results via their respective tree-building algorithms. All authors also helped proof-read the paper.
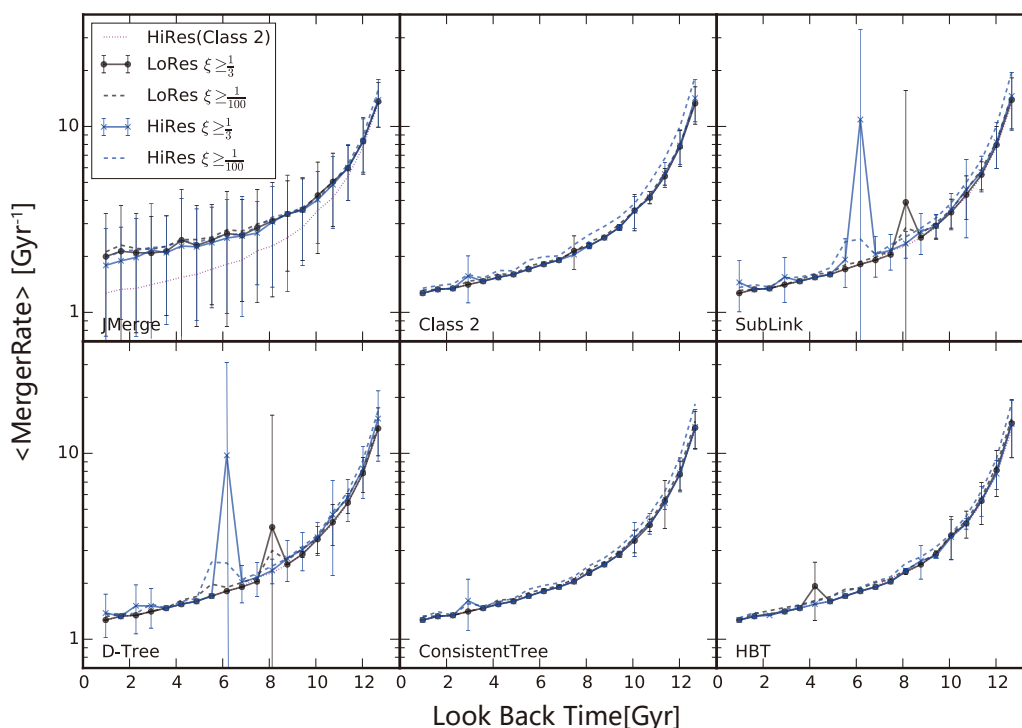
**Figure 14.** Mean merger rate (mergers per descendant halo per Gyr) as a function of look back time. Lines with different colour represent the merger trees built in the LoRes and HiRes simulations, as shown by the legend. Solid lines show the merger rate with progenitor mass ratio larger than $1/3$. Dashed lines show the merger rate with progenitor mass ratio larger than $1/100$. The HiRes line of Class2 ($\xi \geqslant 1/3$) is reproduced in magenta on all panels for guidance. The error bars show the rms in every time bin. Each subpanel displays results for one tree-builder as indicated, except for the four Class2 finders which are indistinguishable and so all shown on the same subpanel.

## REFERENCES

Avila S., Knebe A., Pearce F. R., Schneider A., Srisawat C., Thomas P. A., Behroozi P., Elahi P. J., Han J., Mao Y.-Y., Onions J., Rodriguez-Gomez V., Tweed D., 2014, MNRAS, 441, 3488

Behroozi P., Knebe A., Pearce F. R., Elahi P., Han J., Lux H., Mao Y.-Y., Muldrew S. I., Potter D., Srisawat C., 2015, arXiv preprint arXiv:1506.01405

Behroozi P. S., Wechsler R. H., Wu H.-Y., 2013, The Astrophysical Journal, 762, 109

Blumenthal G. R., Faber S. M., Primack J. R., Rees M. J., 1984, Nat, 311, 517

Bond J. R., Cole S., Efstathiou G., Kaiser N., 1991, ApJ, 379, 440

Efstathiou G., Silk J., 1983, Fund. Cosmic Phys., 9, 1

Elahi P. J., Thacker R. J., Widrow L. M., 2011, MNRAS, 418, 320

Fakhouri O., Ma C.-P., 2008, Monthly Notices of the Royal Astronomical Society, 386, 577

Fakhouri O., Ma C.-P., 2009, Monthly Notices of the Royal Astronomical Society, 394, 1825

Fakhouri O., Ma C.-P., Boylan-Kolchin M., 2010, Monthly Notices of the Royal Astronomical Society, 406, 2267

Genel S., Bouché N., Naab T., Sternberg A., Genzel R., 2010, The Astrophysical Journal, 719, 229

Genel S., Genzel R., Naab T., Sternberg A., et al., 2009, The Astrophysical Journal, 701, 2002

Gill S. P. D., Knebe A., Gibson B. K., Dopita M. A., 2004, MNRAS, 351, 410

Han J., Jing Y. P., Wang H., Wang W., 2012, MNRAS, 427, 2437

Jiang L., Helly J. C., Cole S., Frenk C. S., 2014, MNRAS, 440, 2115

Jung I., Lee J., Yi S. K., 2014, ApJ, 794, 74

Knollmann S. R., Knebe A., 2009, ApJS, 182, 608

Lacey C., Cole S., 1993, MNRAS, 262, 627

Lee J., Lemson G., 2013, J. Cosm. & Astropart. Phys., 5, 22

Lee J., Yi S. K., Elahi P. J., Thomas P. A., Pearce F. R., Behroozi P., Han J., Helly J., Jung I., Knebe A., Mao Y.-Y., Onions J., Rodriguez-Gomez V., Schneider A., Srisawat C., Tweed D., 2014, MNRAS, 445, 4197

Press W. H., Schechter P., 1974, ApJ, 187, 425

Rodriguez-Gomez V., Genel S., Vogelsberger M., Sijacki D., Pillepich A., Sales L. V., Torrey P., Snyder G., Nelson D., Springel V., Ma C.-P., Hernquist L., 2015, MNRAS, 449, 49

Roukema B. F., Quinn P. J., Peterson B. A., Rocca-Volmerange B., 1997, MNRAS, 292, 835

Springel V., 2005, MNRAS, 364, 1105

Springel V., Wang J., Vogelsberger M., Ludlow A., Jenkins A., Helmi A., Navarro J. F., Frenk C. S., White S. D., 2008, MNRAS, 391, 1685

Springel V., White S. D. M., Tormen G., Kauffmann G., 2001, MNRAS, 328, 726

Srisawat C., Knebe A., Pearce F. R., Schneider A., Thomas P. A., Behroozi P., Dolag K., Elahi P. J., Han J., Helly J., Jing Y., Jung I., Lee J., Mao Y.-Y., Onions J., Rodriguez-Gomez V., Tweed D., Yi S. K., 2013, MNRAS, 436, 150

Tweed D., Devriendt J., Blaizot J., Colombi S., Slyz A., 2009, A&A, 506, 647

White S. D. M., Rees M. J., 1978, MNRAS, 183, 341

This paper has been typeset from a TEX/ LATEX file prepared by the author.